MOLECULAR IMAGING AND BIOLOGY

Mol Imaging Biol (2012)
DOI: 10.1007/s11307-012-0561-3

RESEARCH ARTICLE

Imaging of Protein Synthesis: *In Vitro* and *In Vivo* Evaluation of ^{44}Sc-DOTA-Puromycin

Sebastian Eigner,[1] Denis R. Beckford Vera,[1] Marco Fellner,[2] Natalia S. Loktionova,[2] Markus Piel,[1] Ondrej Lebeda,[1] Frank Rösch,[2] Tobias L. Roß,[2] Katerina Eigner Henke[1]

[1]*Nuclear Physics Institute, Department of Radiopharmaceuticals, Academy of Science of the Czech Republic, Husinec-Rez 289, 25068 Husinec-Rez, Czech Republic*

[2]*Institute for Nuclear Chemistry, Johannes Gutenberg-University, Mainz, Germany*

Abstract

Purpose: The purpose of this study was to investigate whether ^{44}Sc-labeled puromycin can be utilized for imaging of protein synthesis *in vivo*.

Methods: For micro-positron emission tomographic (μPET) studies, 20–25 MBq of [^{44}Sc]-DOTA-puromycin was administered to tumor-bearing rats, and animals were scanned for 1 h dynamically. Results were further validated by dissecting organs and tissues of the animals after the measurement and *in vitro* blocking experiments using puromycin or cycloheximide to block protein synthesis.

Results: μPET images of tumor-bearing rats showed significant tumor uptake of [^{44}Sc]-DOTA-puromycin and a clear-cut tumor visualization. In both blocking experiments, cellular uptake of [^{44}Sc]-DOTA-puromycin ([^{44}Sc]-DOTA-Pur) could be suppressed by blocking protein synthesis.

Conclusions: We report for the first time successful μPET imaging with ^{44}Sc obtained from a ^{44}Ti/^{44}Sc generator, as well as noninvasive μPET imaging of ribosomal activity, respectively protein synthesis, with a puromycin-based radiopharmaceutical and the direct correlation between cellular uptake of [^{44}Sc]-DOTA-Pur and protein synthesis.

Key words: Protein synthesis, Scandium-44, DOTA-Pur, Therapy control, μPET, Preclinical imaging

Introduction

Puromycin has played an important role in our understanding of the eukaryotic ribosome and protein synthesis. It has been known for more than 40 years that this antibiotic is a universal protein synthesis inhibitor that acts as a structural analog of an aminoacyl-transfer RNA (aa-tRNA) [1] in eukaryotic ribosomes. In 1964, Nathans [2] demonstrated that the eukaryotic ribosome mistakenly inserts puromycin in place of aa-tRNA, resulting in truncated proteins containing the drug at their C termini. In a later examination of this mechanism, Miyamoto-Sato *et al*. concluded that puromycin inhibits translation solely through C-terminal labeling of peptides and not through additional pathways [3]. This classic model for puromycin action admits only a single mode of action, which is the covalent attachment to the nascent peptide chain [4].

Due to the role of DNA damage-repair enzymes and their synthesis in situations of need (DNA damage, *e.g.*, after chemo- or radiation therapy), determination of protein synthesis is important for control of anti-tumor-therapy, to enhance long-time survival of tumor patients and minimize therapy-caused side effects. Multiple attempts to reach this goal have been made through the last decades, using mostly radiolabeled amino acids, with limited or unsatisfactory success [5]. The difficulties in utilizing radiolabeled amino

This study forms a part of the dissertations of S. Eigner and D. R. Beckford Vera.

Correspondence to: Sebastian Eigner; *e-mail:* eigner@ujf.cas.cz

Published online: 08 May 2012

acids for *in vivo* determination of protein synthesis are due to the wide variety of possible metabolic pathways of amino acids [5].

Puromycin–deoxy-cytidine-conjugates (puromycin–dC-conjugates) labeled with biotin have been utilized by molecular biologists to determine *in vivo* protein synthesis during the last years [3, 4, 6]. Their metabolism has been proven to be only involved in protein synthesis mimicking aa-tRNA. We decided to replace the biotin, which is used as fluorescent dye for detection, with the chelator DOTA (1,4,7,10-tetraazacyclododecane-1,4,7,10-tetraacetic acid). Both molecules are inserted to the puromycin-precursors as activated *N*-hydroxysuccinimide esters.

In this context, positron-emitting radiometals like ^{68}Ga or ^{44}Sc are needed. While the short half-life of ^{68}Ga permits the application of suitable ^{68}Ga activities maintaining an acceptable radiation dose to the patient, it limits application of ^{68}Ga-labeled tracers to the investigation of fast biological processes.

Regarding the fact that protein synthesis is a rather slow process, positron emitters with longer physical half-life are needed, such as ^{44}Sc ($T_{1/2}$=3.97 h) derived from a ^{44}Ti/^{44}Sc generator [7]. ^{44}Sc decays almost entirely by β^+ emission (94.3 %) which is accompanied by emission of 1,157.0 keV photons (99.9 %).

Consequently, the purpose of this study was to investigate whether ^{44}Sc-labeled puromycin-based DOTA-conjugates can be utilized for imaging of protein synthesis *in vivo*.

Material and Methods

Equipment and Reagents

DOTA-NHC$_6$-dC-puromycin (DOTA-Pur) (Fig. 1) was purchased from Purimex (Grebenstein, Germany). Chelex 100 in sodium form and human serum albumin were purchased from Sigma (Steinheim, Germany). All other reagents were purchased from Merck (Darmstadt, Germany) or Fluka (Steinheim, Germany) with the highest purity available. Ultrapure water (Aquatec Water Systems, Inc., CA, USA) was used for all procedures. To avoid metal contamination, all solutions used in conjugation and radiolabeling reactions were passed through a Chelex 100 column (1×10 cm). All glassware was washed with 2 M HCl and ultrapure water.

^{44}Sc Production

^{44}Sc was produced via a ^{44}Ti/^{44}Sc generator as described previously by Loktionova *et al*. [8]. Online processing was carried out adsorbing ^{44}Sc on a cationic resin AG 50W-X8 (200–400 mesh, H^+-form) with ≥98 % efficacy. The purified ^{44}Sc was desorbed by using 3 ml of 0.25 M ammonium acetate (NH_4OAc), pH=4.0 [9], ready for labeling.

Synthesis of DOTA-NHC$_6$-dC-puromycin (DOTA-Pur)

DOTA-Pur was synthesized using a puromycin-tethered CPG support by the usual protocol for automated DNA and RNA synthesis (phosphoramidite method [4]) following our design by Purimex (Grebenstein, Germany). The compound was purified by Purimex using reversed-phase high-performance liquid chromatography (HPLC) and desalted. DOTA-Pur was used without any further purification in our experiments, since initial control of the compound via HPLC showed a chemical purity of more than 98 %. The purity of DOTA-Pur was reported to be higher than 98 % after double purification using reversed-phase HPLC (Fig. 2). DOTA-Pur was used without further purification.

[^{44}Sc]-Radiolabeling of DOTA-Pur

Fifty microliters DOTA-Pur in H_2O (1.11 nmol/ µl) was added directly to the eluate from the generator (3 ml of 0.25 M NH_4OAc, pH=4.0) containing ~150 MBq ^{44}Sc and incubated in a heating block at 95°C for 20 min while shaking. The reaction mixture was loaded into a reversed-phase C-18 cartridge (Strata-X 33 µm Polymeric Sorbet 60 mg/ml. Phenomenex, Inc. USA). The cartridge was washed with 2 ml of H_2O to eluate the free ^{68}Ga. [^{44}Sc]-DOTA-puromycin ([^{44}Sc]-DOTA-Pur) was eluted from the resin in 300 µl ethanol. The ethanol was then evaporated by heating the eluate, and the product redissolved in 0.9 % saline to a final radioactive concentration of 30 MBq/ml. Radiolabeling efficiency and radiochemical purity were determined by thin-layer chromatography performed on SG-TLC plates (Pall Corporation, USA), using *n*-propanol/NH_4OH/H_2O (55:35:10) as the mobile phase. Radiation counting of thin-layer chromatography (TLC) plates was performed with a Cyclone Plus Storage Phosphor System (Perkin Elmer, USA).

In Vitro Studies

All described *in vitro* studies were carried out in DU145 (HTB-81™: human prostate carcinoma) and BJ (CRL-2522™: human foreskin fibroblasts) cells. Cells have been purchased between 2 and 4 months before conducting the experiments. Cells are commercially available at LGC/ATCC, Lomianki, Poland.

In Vitro Uptake and Protein Incorporation

DU145 and BJ cells were routinely cultivated in standardized supplemented full media (Roswell Park Memorial Institute medium formulation 1640 (RPMI 1640)+10 % fetal calf serum (FCS)+1 % penicillin/streptomycin (PAA, Czech Republic)) at 37°C in a humidified atmosphere containing 5 % CO_2. Cell preparation for the experiments was carried out 48 h before hand, seeding 2×10^5 living cells per well in six-well-plates (Becton, Dickinson and Company, USA) using 2 ml of normal media. Therefore, cells were harvested by trypsinization, and the number of living cells was determined utilizing a CASY TT-Cell Analyzing System (Innovatis, Reutlingen, Germany). During the experiments, the number of living cells was counted for each measurement using CASY TT. All data were normalized to 1×10^6 living cells.

Total cellular uptake was measured after incubation of the cells with 84 pmol [^{44}Sc]-DOTA-Pur per well for 2 h. Incubation was stopped by discarding the treatment media and washing the cells twice with ice-cold PBS. In the next step, cells were dissolved in 500 µl lysis-buffer (10 % NaOH+5 % sodium dodecyl sulfate), and the total sample activity was measured in a fully automated gamma counter (2470 Wizard^2, Perkin Elmer, USA). For measuring the protein

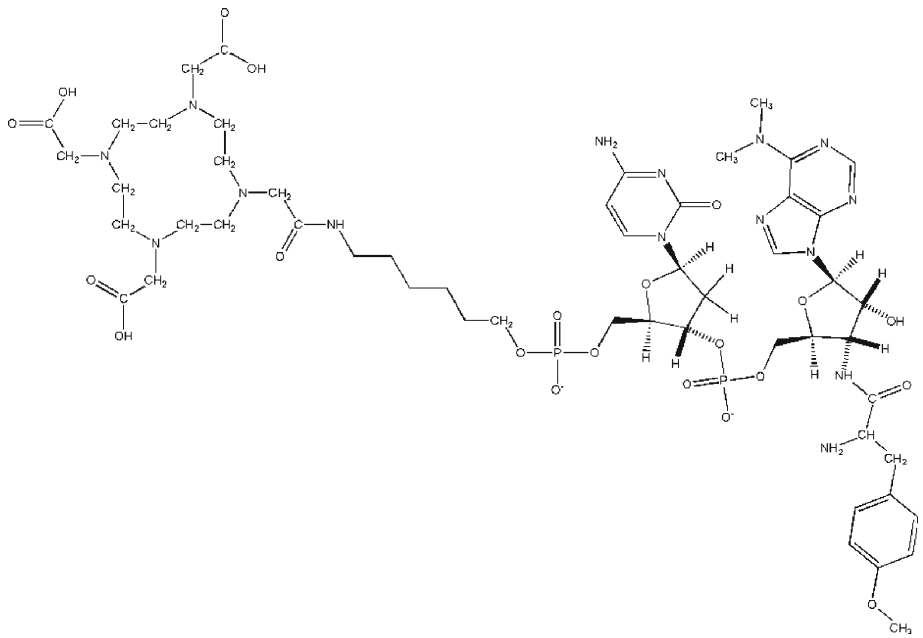

Fig. 1. DOTA-NHC$_6$-dC-puromycin—DOTA-NHC$_6$-deoxycytidine-puromycin—was produced at Purimex (Grebenstein, Germany) analog to the biotin derivatives developed by Starck et al. (puromycin-2P) [4].

incorporation, proteins were then precipitated and isolated by addition of trichloroacetic acid (TCA) to a final concentration of ≥10 %. After centrifugation, the supernatant was removed and the precipitate washed twice with TCA solution. Activity contained in the acid solution and protein pellet was determined in the automated gamma-counter. Results were calculated using GraphPad Prism software (GraphPad Software, Inc., California, USA).

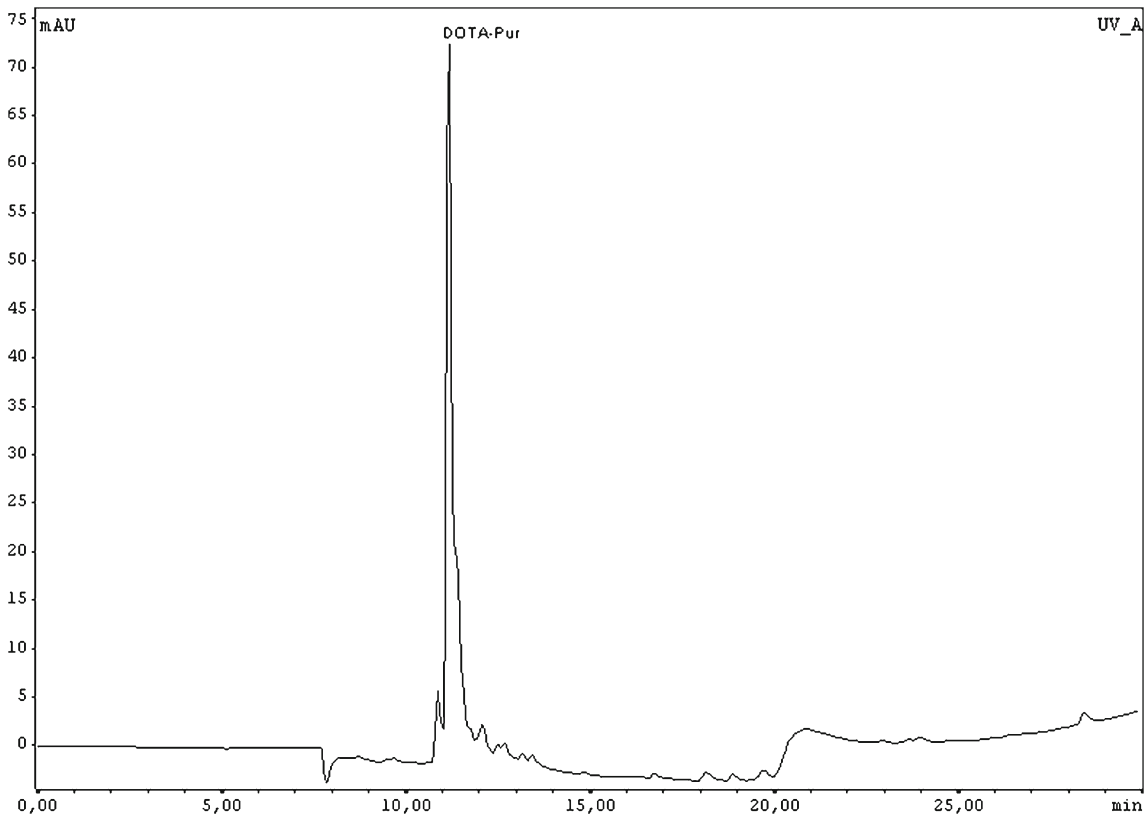

Fig. 2. HPLC-chromatogram of DOTA-Pur—solvent A, 0.1 % trifluoracetic acid (TFA)/H_2O; solvent B, 0.1 % TFA/acetonitrile; gradient elution, 0 min, 80 % B–20 % C; 30 min, 60 % B–40 % C.

Inhibition of [^{44}Sc]-DOTA-Pur Incorporation into Proteins

Experiments using distinct inhibitors of protein synthesis were carried out in six-well-plates (Becton, Dickinson and Company, USA), 2×10^5 cells/well—a competitive inhibition using puromycin dihydrochloride (puromycin) (P9620, Sigma, Steinheim, Germany) and a non-competitive inhibition using 3-[2-(3,5-dimethyl-2-oxo-cyclohexyl)-2-hydroxyethyl] glutarimide (cycloheximide) (Fluka, Steinheim, Germany) as inhibitors.

The competitive effect of puromycin is due to competition with the puromycin-conjugate for free ribosomal A-sites (competitive inhibition). Experiments were carried out to evaluate whether puromycin and puromycin-conjugates still use the same mechanism of action for inhibition of protein synthesis. Cycloheximide exerts its effect by interfering with the translocation step in protein synthesis (movement of two tRNA molecules and mRNA in relation to the ribosome) thus blocking translational elongation.

DU145 and BJ cells were treated simultaneously with 84 pmol/well of [^{44}Sc]-DOTA-Pur and inhibitor concentrations between 10 pmol/well and 20 nmol/well. Cells were incubated for 1 h, and total cellular uptake was measured as described above. Results were calculated as response in percent of non-competed uptake and plotted semi-logarithmic against concentration of inhibitor using GraphPad Prism software (GraphPad Software, Inc., California, USA).

µPET Imaging in Tumor-Bearing Rats

All used cell lines and animals were provided by the Institute of Physiology, Johannes Gutenberg-University Mainz, Germany. Rat cell lines AT1 (sub-line of Dunning R3327 rat prostate carcinoma) and Walker carcinoma 256 (subcutaneous solid tumor) were used in all experiments. AT1 cells were grown in RPMI 1640 medium supplemented with 10 % FCS and Walker cells in Dulbecco's modified Eagle medium (Gibco no. 430–1600, Gibco, Darmstadt, Germany) containing 5 % FCS, 2.5 µg/ml amphotericin B, 50 µg/ml kanamycin, 100 µg/ ml streptomycin, and 100 U/ ml penicillin at 37°C under a humidified 5 % CO_2 atmosphere. Medium was changed routinely every 2 days, and passages were done once a week.

For tumor implantation with AT1 cells, male Copenhagen rats (Charles River Wiga, Sulzfeld, Germany; body weight 150–200 g) and with Walker cells male CD(SG)IGS rats (Charles River Wiga, Sulzfeld, Germany; body weight 150–200 g) were used, respectively. Animals were housed in the animal care facility of the Johannes Gutenberg-University Mainz and allowed for access to food and water *ad libitum* before the investigation. All experiments had previously been approved by the regional Animal Ethics Committee and were conducted in accordance with the German Law for Animal Protection and the UK Coordinating Committee on Cancer Research (UKCCCR) Guidelines [9]. Solid carcinomas of both cell lines were heterotopically induced by injection of the cells (0.4 ml, 10^4 cells/µl) subcutaneously into the dorsum of the hind foot. Tumors grew flat, solid, and spherical. Volumes were determined by measuring the three orthogonal diameters (d) of the tumors and using an ellipsoid approximation with the formula: $V=(\pi/6)\times d_1\times d_2\times d_3$. Animals were used for micro-positron emission tomographic (µPET) studies when the tumors reached volumes between 1.0 and 2.0 ml, approximately 10–14 days after tumor cell inoculation.

The µPET imaging was performed on a µPET Focus 120 small animal PET (Siemens/Concorde, Knoxville, TN, USA). During PET measurements, anesthetized (3 % isoflurane in oxygen) animals (230–270 g body weight) were placed tail first supine in the field of view. To keep body temperature of the animals stable, an infrared light source was placed near the animals. The 20–25 MBq of [^{44}Sc]-DOTA-puromycin in 0.4–0.7 ml 0.9 % NaCl solution was administered as a bolus via a previously inserted catheter in the tail vein while the animals were already placed inside the µPET.

Time–activity curves (TAC) were obtained with varying time frames (1–5 min) for a total measuring interval of 60 or 120 min. The PET list-mode data were histogrammed into 15 frames and reconstructed using interlaced ordered subset expectation maximization (OSEM 2d) algorithm. Volumes of interest were defined for tumor and reference tissue (testis). Tissue concentration in testis was nearly constant for all animals on a low level indicating low tracer uptake. Ratios of tumor to reference tissue were calculated from TAC. Optical reconstruction and estimation of TAC was performed using PMOD (PMOD Technologies Ltd., Zürich, Switzerland)

Biodistribution in Tumor-Bearing Rats

After 120 or 240 min polarization index (p.i.), anesthetized rats were killed by cervical dislocation. After partial removal of different organs, biodistribution of [^{44}Sc]-DOTA-Pur in this tissues (blood, liver, kidneys spleen, heart, lung, femur with bone marrow, tumors, brain, and testis) was estimated using an automate gamma-counter. Organ uptakes were than calculated in percent of injected does per gram tissue. Results were calculated and plotted using GraphPad Prism software (GraphPad Software, Inc., California, USA).

Statistical Analysis

Quantitative data were expressed as mean±SD. Means were compared using Student's t test; p values less than 0.05 were considered statistically significant.

Results

^{44}Sc-Labeling of DOTA-Pur

In the TLC system used for radiolabeling efficiency and radiochemical purity determination, free ^{68}Ga remained in the start while ^{68}Ga-DOTA-Pur migrated to the front. Radiochemical purity determined by TLC before purification of the reaction mixture was 78±2 %. After purification, the radiochemical purity exceeded 97 % in all preparations (Fig. 3). Overall recovery after purification on reversed-phase C-18 cartridges was 59.0±6.0 %. Specific activity of purified [^{44}Sc]-DOTA-Pur was 1.5±0.1 GBq/µmol.

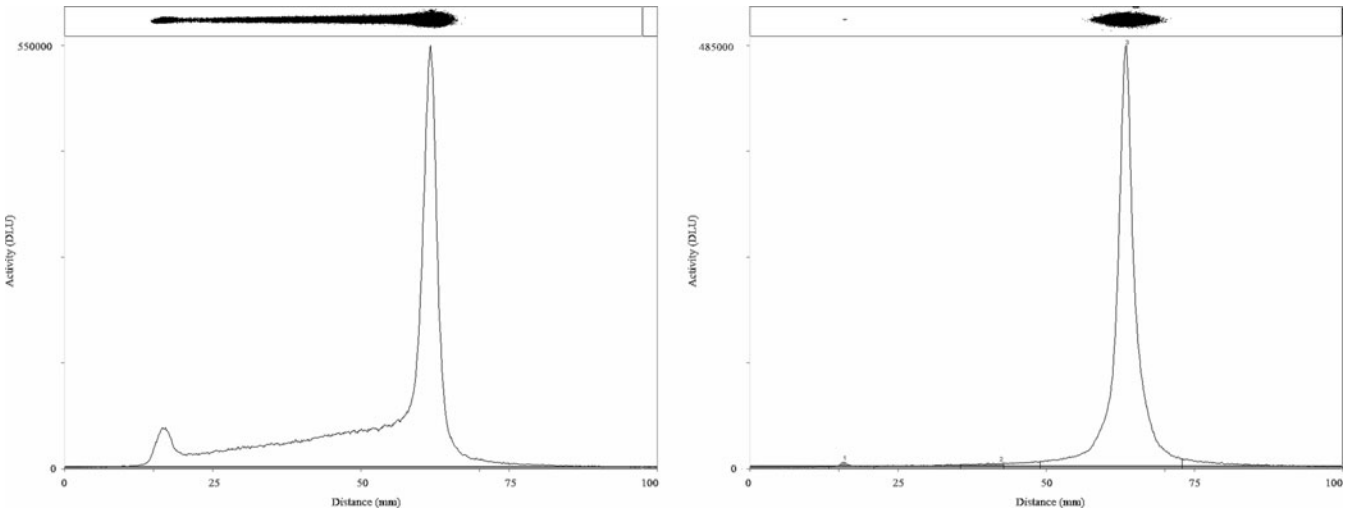

Fig. 3. Instant thin-layer chromatograms (iTLC) of reaction mixture and purified product in 0.9 % saline solution; radiochemical purity after purification ≥97 %.

In Vitro Uptake and Protein Incorporation

Uptake in tumor cells (DU145) after 2 h was 2.0±0.1 % of the applied dose per 1×10^6 cells; in normal skin fibroblasts, it was 0.2±0.1 % applied dose per 1×10^6 cells. Tumor-to-normal-cell ratio was approximately 10:1. Protein incorporation after 2 h in tumor and normal cell line was ≥93 % of the uptake and was 2.0±0.1 % of applied dose per 1×10^6 cells for tumor cells and 0.2±0.1 % per 1×10^6 cells for normal cells.

Inhibition of [^{44}Sc]-DOTA-Pur Incorporation into Proteins

While the mechanism of action of the two inhibitors is completely different, addition of both resulted in reducing cellular uptake to normal cell level. Irreversible competitive inhibition with puromycin decreased cellular uptake of DU145 tumor cells to less than 0.2±0.1 % (8.2±0.2 % of initial uptake values) when adding ≥200 pmol of the inhibitor (Fig. 4a). Inhibition of protein synthesis utilizing cycloheximide for non-competitive inhibition reduced the cellular uptake of [^{44}Sc]-DOTA-Pur to ≤0.3±0.1 % (12.1±0.2 % of initial uptake values) when adding ≥200 pmol of the inhibitor (Fig. 4b).

μPET Imaging in Tumor-Bearing Rats

To show the feasibility of DOTA-Pur for imaging of protein synthesis in tumors, [^{44}Sc]-DOTA-Pur was injected intravenously into Walker carcinoma and AT1 tumor-bearing rats, and μPET scans were performed from 0 to 60 or 120 min p.i. Summed image of Walker carcinoma from 3 to 20 min and tumor as well as reference tissue TAC from 0 to 60 min p.i. obtained from dynamic scans are shown in Fig. 5. Summed image of AT1 tumors from 3 to 20 min and tumor as well as reference tissue TAC from 0 to 60 min p.i. obtained from dynamic scans are shown in Fig. 6. Both tumors are clearly visualized with high tumor-to-background contrast (≥40:1). Highest tumor uptake was measured between 3 and 6 min p.i.. Most of the AT1 tumors showed necrotic tissue inside the tumor when removed for *ex vivo* biodistribution. The necrotic regions of the tumors are clearly visible inside the tumor outlines (arrowheads in

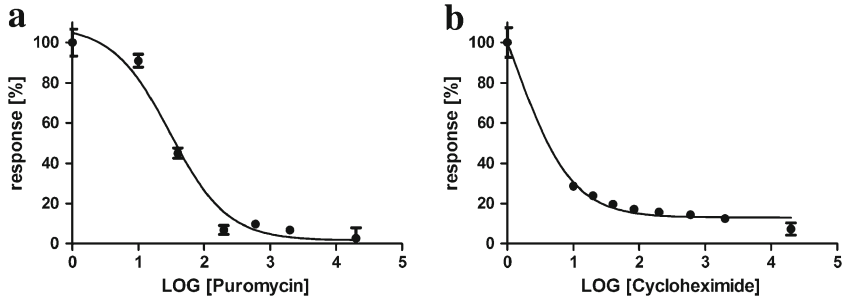

Fig. 4. **a** Competitive inhibition of [^{44}Sc]-DOTA-Pur uptake using increasing concentrations from 10 to 20 nmol/well of puromycin dihydrochloride. Reduction of cellular uptake to normal cell level from ≥200 nmol/well; **b** Non-competitive inhibition of [^{44}Sc]-DOTA-Pur uptake using increasing concentrations from 10 to 20 nmol/well of cycloheximide. Reduction of cellular uptake to normal cell level from ≥200 nmol/well.

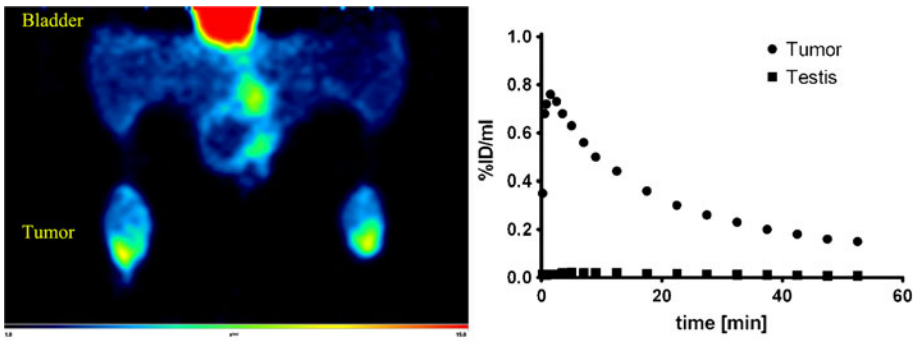

Fig. 5. Summed μPET-image, coronal slice, colors expressed as SUV (0–12) (3–20 min, dynamic scan) of Walker carcinomas on hind feet of CD rats and TAC 0–60 min of tumor and testis (reference). Obtained TAC looks like cell uptake and slow wash-out caused by retention of the [^{44}Sc]-DOTA-Pur as aa-tRNA-analog within eukaryotic ribosomal A-site.

Fig. 6). Prominent activity is located in the kidneys and urinary bladder, the major excretion pathway of DOTA-Pur. The 120 min TAC revealed a steady state for tumor uptake after 65 to 70 min (Fig. 7a).

Biodistribution in Tumor-Bearing Rats

The biodistribution data for tumor-bearing rats showed low uptake in normal tissue, and a tumor-to-non-tumor ratio of 6:1 was found after 2 h and 9:1 after 4 h. Major excretion route was via the renal system. More than 95 % of the injected dose was cleared from the organism after 2 h.

Discussion

Synthesis of proteins is a fundamental process for all cellular functions. Because of the uncontrolled and accelerated growth of cancer, the process of protein synthesis in tumors is increased. As a consequence, the demand of proteins, the building blocks of cellular structures and enzymes, is increased. Therefore, it is expected that radiolabeled amino acid tracers will also accumulate in tumors. In brain tumor imaging, the use of radiolabeled amino acids is quite well established. In most other tumors, the data are not sufficient to permit definitive conclusions [5, 10].

Amino acid tracers were initially developed with the intention to measure protein synthesis rates. However, the rate of amino acid transport rather than the protein synthesis rate seems to be the major determinant of tracer uptake in tumor imaging studies. This study showed that suitably labeled puromycin conjugates can be used to image eukaryotic ribosomal activity and therefore protein synthesis in preclinical animal models. In particular, this study demonstrated that Walker carcinomas and AT1 tumors have protein synthesis-specific accumulation of [^{44}Sc]-DOTA-Pur. The tumor uptakes in this study are comparable with those obtained utilizing $^{67/68}$Ga-labeled [desferrioxamine B (DFO)]-octreotides or *N*-[*N*-[(*S*)-1,3-dicarboxypropyl]-carbamoyl]-*S*-[^{11}C]methyl-L-cysteine and *N*-[*N*-[(*S*)-1,3-dicarboxypropyl]carbamoyl]-*S*-3-[^{125}I]iodo-L-tyrosine [11, 12]. Tumor-to-background ratios are higher than 30:1.

The most important biochemical property to be tested of an analog tracer for the assessment of protein synthesis *in vivo* is its acceptance by the ribosomal A-site and aa-tRNA synthetase and its subsequent incorporation into peptide chains by ligase enzyme systems. The generally applied method of isolating proteins from tissue homogenates by TCA precipitation is rather crude. It especially does not discriminate between real incorporation into the peptide chain and possible binding as false substrate to one or several enzymes, with which it would be co-precipitated by

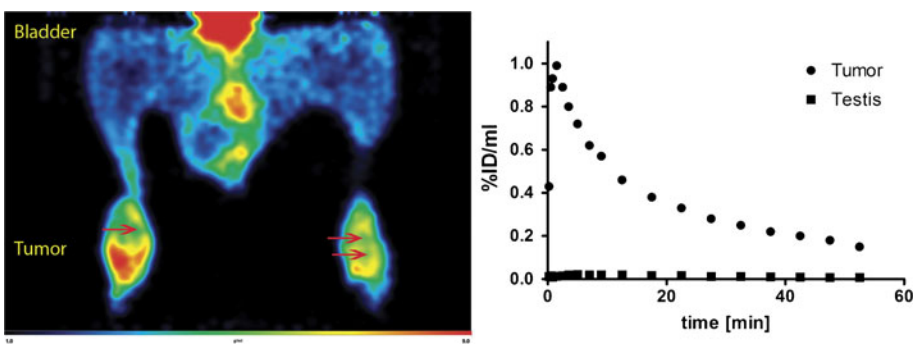

Fig. 6. Summed μPET image, coronal slice, colors expressed as SUV (0–9) (3–20 min, dynamic scan) of AT1 tumors on hind feet of Copenhagen rats and TAC 0–60 min of tumor and testis (reference); *red arrows* indicate necrotic tissue within the visible tumor outlines (approved by tumor resection after end of scans).

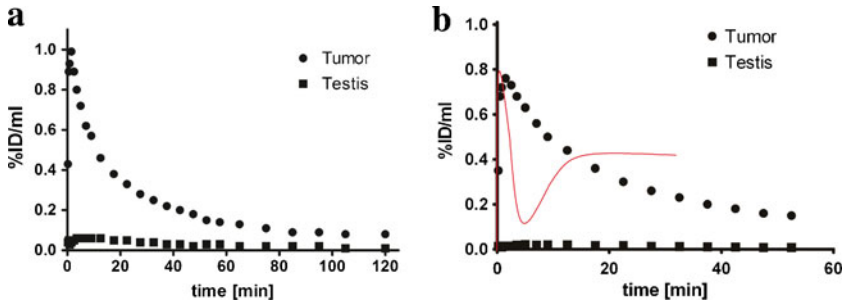

Fig. 7. **a** 0–120 min TAC of tumor and testis (reference) of AT1 tumor on hind feet of Copenhagen rats; steady state reached after approximately 65 min; **b** TAC of DOTA-Pur derivatives with prolonged half-life in blood are expected to look like the *red curve* (manually inserted), due to protein incorporation and trapping.

TCA. Since it has been demonstrated by Nathans [2] and Smith *et al*. [13] that there is only one possible pathway for puromycin and puromycin-conjugates inside cells, this method can be applied to determine exactly the protein bound fractions of [^{44}Sc]-DOTA-Pur.

As the protein-bound fraction after 2 h is ≥93 % of the cellular uptake, a direct dependency of the uptake on the protein incorporation ratio is of the essence. Both blocking experiments, performed on eukaryotic tumor cells, showed significant reduction of the cellular uptake to the level of normal cells which were used as reference. Therefore, the visible accumulation of activity in tumors is due to be equivalent with the amount of active ribosomes and therefore, protein synthesis, in the region of interest.

^{44}Sc exhibits several attractive properties as a PET nuclide such as its excellent availability by the ^{44}Ti/^{44}Sc-generator and its convenient half-life of 3.9 h. Since it can be obtained from the generator-based system, ^{44}Sc represents an attractive alternative to cyclotron-based PET radiopharmaceuticals [8, 9]. The labeling efficiency of [^{44}Sc]-DOTA-Pur and the overall recovery was between 55 % and 65 %, which still presents opportunity for improvement but is comparable to labeling yields for DOTA-derivatives of peptides and oligo-nucleotides labeled with ^{68}Ga. The same goes for the specific activity of the purified compound [14, 15].

TAC and *ex vivo* biodistribution studies revealed that, after 1 h, more than 95 % of the injected activity has been excreted via the renal system. Since protein synthesis is a rather slow process, it will be necessary to prolong the half-life in blood for further improvement of tumor accumulation of DOTA-Pur, which results in a classical increase of activity inside the tumor over time (Fig. 7b: red line). Shelly *et al*. [4] showed that puromycin-oligonucleotides reveal steric restrictions for ribosome entry and multiple modes of translation inhibition. Therefore, changes in the structure of the conjugate might result in decreasing the biological activity of the modified molecule. Even if the half-life in blood will be prolonged due to modifications, it might result in decreased ribosomal acceptance and thus in reduced accumulation of the puromycin-conjugate in tumor tissue.

Due to the cytotoxicity of puromycin administered in ≥1 mmol concentrations (resulting in non-functional protein fragments), increasing the dose to achieve an increased amount of protein incorporation is not an option.

Since ribosomal activity only can be found during protein synthesis, the determination of ribosomal activity is a direct equivalent for protein synthesis. The more active ribosomes are present, the higher the retention of [^{44}Sc]-DOTA-Pur in the cell, as shown in the blocking experiments utilizing cycloheximide and puromycin.

Fluorescence-labeled puromycin derivatives are used in molecular biology for the last two decades to determine protein synthesis *in vivo*. Since optical imaging of fluorophores like biotin in tissue is limited due to a tissue penetration of 0.5–2.0 cm at maximum, the use for diagnostics in human beings is not applicable. Since penetration depth and attenuation of light photons and 0.5 MeV photons from PET radiopharmaceuticals differ significantly, the radiolabeled DOTA-puromycin-conjugate allows for high resolution and precise quantification and is thus superior to any optic-photon-based imaging agent.

Taking all these facts into account, the most suitable possibility for increasing the half-life in blood might be the use of infusion pumps for administration of a steady dose over time instead of application in a bolus injection.

Conclusions

We report for the first time successful μPET imaging with ^{44}Sc obtained from a ^{44}Ti/^{44}Sc generator. [^{44}Sc]-DOTA-Pur showed very high tumor-to-background ratios in two subcutaneous tumor models. The results demonstrated mainly renal excretion and rapid blood clearance. Activity accumulation in the tumors reached an early maximum. Tumor-to-muscle contrast was positive at all times. This study further revealed that optimization of the tracer to obtain prolonged tumor uptake and half-life in blood to improve *in vivo* kinetics as well as improvements in labeling and purification are needed. We anticipate that non-invasive studies of protein synthesis via ribosomal activity using PET can become an important tool for therapy control and target identification for therapy. We demonstrated that ^{44}Sc-labeled puromycin-based DOTA-conjugates can be utilized for

imaging of ribosomal activity and hence protein synthesis *in vivo*.

Acknowledgments. This project was subsidized by the Ministry of Education, Youth and Sports of the Czech Republic: Project NPV II 2B06165.

We thank Dr. Nicole Bausbacher, Department of Nuclear Medicine, University Medicine, Mainz, Germany, and Barbara Biesalski for outstanding support on μPET imaging.

We thank Dr. Matthias Miederer, Department of Nuclear Medicine, University Medicine Mainz, Germany, for his support in fulfilling the requirements of the national animal protection laws.

Conflicts of interest. None.

References

1. Yarmolinsky MB, Haba GL (1959) Inhibition by puromycin of amino acid incorporation into protein. Proc Natl Acad Sci (USA) 45(12):1721–1729
2. Nathans D (1964) Puromycin inhibition of protein synthesis: incorporation of puromycin into peptide chains. Proc Natl Acad Sci (USA) 51:585–592
3. Miyamoto-Sato E, Nemoto N, Kobayashi K et al (2000) Specific bonding of puromycin to full-length protein at the C-terminus. Nucleic Acids Res 28(5):1176–1182
4. Starck SR, Roberts RW (2002) Puromycin oligonucleotides reveal steric restrictions for ribosome entry and multiple modes of translation inhibition. RNA 8:15
5. Haubner R (2010) PET radiopharmaceuticals in radiation treatment planning—synthesis and biological characteristics. Radiother Oncol 96 (3):280–287
6. Nemoto N, Miyamoto-Sato E, Yanagawa H (1999) Fluorescence labeling of the C-terminus of proteins with a puromycin analogue in cell-free translation systems. FEBS Lett 462(1–2):43–46
7. Rösch F, Knapp F (eds) (2004) Radionuclide generators. The Netherlands: Kluwer Academic Publishers. vol. 4, p 81–118
8. Filosofov DV, Loktionova NS, Rösch F (2010) A 44Ti/44Sc radionuclide generator for potential application of 44Sc-based PET-radiopharmaceuticals. Radiochim Acta 98(3):149–156
9. Pruszyński M, Loktionova NS, Filosofov DV et al (2010) Post-elution processing of 44Ti/44Sc generator-derived 44Sc for clinical application. Appl Radiat Isot 68(9):1636–1641
10. Jager PL, de Korte MA, Lub-de Hooge MN et al (2005) Molecular imaging: what can be used today. Cancer Imaging 5(Spec No A):S27–S32
11. Smith-Jones PM, Stolz B, Bruns C et al (1994) Gallium-67/gallium-68-[DFO]-octreotide—a potential radiopharmaceutical for PET imaging of somatostatin receptor-positive tumors: synthesis and radiolabeling *in vitro* and preliminary *in vivo* studies. J Nucl Med 35(2):317–325
12. Foss CA, Mease RC, Fan H et al (2005) Radiolabeled small-molecule ligands for prostate-specific membrane antigen: *in vivo* imaging in experimental models of prostate cancer. Clin Cancer Res 11(11):4022–4028
13. Smith J, Traut R, Blackburn G et al (1965) Action of puromycin in polyadenylic acid-directed polylysine synthesis. J Mol Biol 13:617–628
14. Meyer GJ, Macke H, Schuhmacher J et al (2004) 68Ga-labelled DOTA-derivatised peptide ligands. Eur J Nucl Med Mol Imaging 31(8):1097–1104
15. Roivainen A, Tolvanen T, Salomaki S et al (2004) 68Ga-labeled oligonucleotides for *in vivo* imaging with PET. J Nucl Med 45(2):347–355